

SuperMatching: Feature Matching using Supersymmetric Geometric Constraints

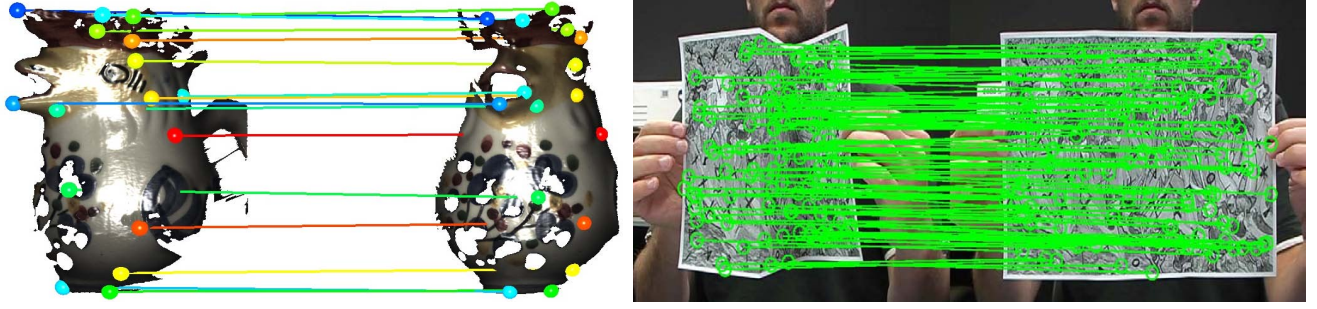


Figure 1: Correspondences between datasets determined by SuperMatching, using feature points created by the uniform sampling on the left rigid scans and SIFT feature points on the right deformable surface. For clarity, only some representative matches are shown.

Abstract

Feature matching is a challenging problem lying at the heart of numerous computer graphics and computer vision applications. We present here the *SuperMatching* algorithm for finding correspondences between two sets of features. It does so by considering triangles or higher-order tuples of points, going beyond the pointwise and pairwise approaches typically used. SuperMatching is formulated using a supersymmetric tensor representing an affinity metric which takes into account feature similarity and geometric constraints between features: feature matching is cast as a higher-order graph matching problem. SuperMatching takes advantage of supersymmetry to devise an efficient sampling strategy to estimate the affinity tensor, as well as to store the estimated tensor compactly. Matching is performed by an efficient higher-order power iteration approach which takes advantage of this compact representation. Experiments on both synthetic and real captured data show that SuperMatching provides more accurate feature matching than other state-of-the-art approaches for a wide range of 2D and 3D features, with competitive computational cost.

Keywords: Feature matching; Geometric constraints; Supersymmetric tensor

1 Introduction

Building correspondences between two sets of features belonging to a pair of 2D images or 3D shapes is a fundamental problem in many computer graphics, geometry processing, and computer vision tasks. It arises in applications such as registration of partial or entire 3D shapes [Besl and McKay 1992; Gelfand et al. 2005; Aiger et al. 2008; Li et al. 2008; Chang and Zwicker 2009; Zeng et al. 2010; van Kaick et al. 2011; Chang and Zwicker 2011], shape retrieval from databases [Bronstein et al. 2011], shape matching [Berg et al. 2005; Brown and Rusinkiewicz 2007; Torresani et al. 2008; Tevs et al. 2009; Ovsjanikov et al. 2010; Tevs et al. 2011; Sahillioglu and Yemez 2011; Windheuser et al. 2011], shape reconstruction [Brown and Rusinkiewicz 2007; Pekelný and Gotsman 2008; Wand et al. 2009; Chang and Zwicker 2011], and automatic shape understanding [Huttenlocher and Ullman 1990; Lipman and Funkhouser 2009; Sun et al. 2010; Kim et al. 2011].

Determining correspondences is typically done in three steps [Johnson and Hebert 1999; Lowe 2004; Sun et al. 2009; Toler-Franklin

et al. 2010; Leutenegger et al. 2011]: (i) computing high-quality descriptors which serve to distinguish points from one another, (ii) choosing certain salient points with unusual feature descriptors, for matching, and (iii) determining the most suitable matching between the two sets of points. The former two problems have attracted considerable attention; their importance is clear. However, even supposing ideal feature descriptors and selectors that capture the most important and distinctive information about the neighborhood of each salient point, state-of-the-art algorithms still find it challenging to determine the best matching [van Kaick et al. 2011]: real input data is noisy, and data may only be approximately in correspondence. The problem is further complicated by the presence of symmetric and congruent regions. Various feature matching algorithms have been devised to be robust in the presence of such issues. RANSAC-like algorithms [Tevs et al. 2009; Tevs et al. 2011] minimize the effects of outliers, while generalized multidimensional scaling [Bronstein et al. 2011] and heat kernel maps [Ovsjanikov et al. 2010] consider the manifold in which the points are embedded. Möbius transformations [Lipman and Funkhouser 2009; Kim et al. 2011] also provide a powerful approach. However, these previous algorithms generally do not treat the matching step as an independent problem, even if matching is not tightly coupled with feature description and selection. This paper focuses on the feature matching problem as a problem in its own right.

Matching may be done pointwise (single points to single points), or using tuples of points: e.g. point pairs, separated by a fixed distance, to other point pairs, triples of points forming a triangle to other triples of points, and so on. As pointed out by [Conte et al. 2004], matching single features leads to a linear assignment problem, but if multiple features are matched simultaneously, a quadratic or higher-order assignment problem results. Matching two feature sets by considering similarities of *single* features from each set can easily fail in the presence of ambiguities such as repeated elements, or similar local appearance. Quadratic and higher-order assignment matches groups of features, enforcing other constraints such as consistency of distances between the points in each tuple being matched. Doing so helps to reject many false matches, greatly improving the matching output. Feature similarity and satisfaction of constraints may in general be expressed in terms of an affinity tensor relating pairs of point tuples.

As a particular example of *quadratic* assignment, Leordeanu and Hebert [Leordeanu and Hebert 2005] consider pairs of feature descriptors, and use *distances* between pairs of features from each set to reduce the number of incorrect correspondences. Such pairwise distance constraints are particularly helpful in cases when the fea-

tures themselves have low discriminative ability. The idea has been widely adopted in 3D shape matching algorithms [Tevs et al. 2009; Ovsjanikov et al. 2010; Tevs et al. 2011; Kim et al. 2011; Sahillioglu and Yemez 2011; Windheuser et al. 2011].

Higher-order assignment includes yet more complex constraints between features. For example, third-order potential functions, used in [Duchenne et al. 2009; Zeng et al. 2010; Chertok and Keller 2010; Wang et al. 2010], quantify the affinity between two point triples by measuring the similarity of the angles of the triangles formed by such triples. However, this angular similarity value only considers the *total* difference in corresponding angles, and does not change with reordering of elements in the tuple. When similarity is expressed in this way, the affinity tensor becomes a *supersymmetric* tensor [Kofidis and Regalia 2002].

Our *SuperMatching* algorithm also formulates higher-order matching problems using a supersymmetric affinity tensor. It can accurately match a moderate number of features (several hundreds) using triples or larger tuples of features. The contributions of this paper include:

- We show how to define a compact higher-order supersymmetric affinity tensor to express geometrically consistent constraints between feature tuples.
- Complete computation of the full affinity tensor is computationally infeasible. We efficiently estimate it using a sampling strategy which takes advantage of supersymmetry. This avoids sampling repetitive items, it allows the tensor to be stored compactly, and also improves the matching accuracy by avoiding imbalances in sampling.
- We make full use of the compactness of the affinity tensor to deduce a power iteration method which efficiently solves the matching problem.

Our experiments using both synthetic and real captured data sets show that SuperMatching is more accurate and robust than prior methods, yet has similar computational cost. Importantly, it is a general matching approach, independent of choice of 2D or 3D feature descriptors, feature point selection method, and constraints placed on tuples.

2 Related work

Previous approaches to feature matching can be classified into those which match single points to single points, those which match point pairs to point pairs, and so on.

Matching single points to single points is a linear assignment problem which only considers an affinity measure between two features, one from each set being matched. The affinity measure is typically defined as the feature distance between the feature vectors, which in turn are based on local information around each feature point, e.g. SIFT [Lowe 2004], spin images [Johnson and Hebert 1999], heat diffusion signatures [Sun et al. 2009], and BRISK [Leutenegger et al. 2011]. Point-to-point matching can give misleading results as wrong correspondences are readily established.

Matching point pairs in one set to point pairs in the other set leads to a quadratic assignment problem. Such methods now take into account both similarity of the point features, *and* either the Euclidean distance between the points in a pair, assuming the two sets of points are related by a rigid transformation [Leordeanu and Hebert 2005; Cour et al. 2006], or the geodesic distance, assuming isometry [Li et al. 2008; Tevs et al. 2009; Ovsjanikov et al. 2010; Tevs et al. 2011; Sahillioglu and Yemez 2011; Windheuser et al. 2011].

Unfortunately, this quadratic assignment problem is NP-hard, and again, matches found are not always reliable.

Several higher-order approaches have also been proposed. While they can significantly improve matching accuracy, higher-order assignment is even more computationally demanding, so various approximate methods have been developed. [Zass and Shashua 2008] considered a probabilistic model of soft hypergraph matching. They reduce the higher-order problem to a first-order one by marginalizing the higher-order tensor to a one dimensional probability vector. [Duchenne et al. 2009] introduced the use of a third-order tensor in place of an affinity matrix to represent affinities of feature triples, and higher-order power iteration was used to achieve the final matching. [Wang et al. 2010] built a unified multiple higher-order affinity tensor, by extending the third-order tensor method [Duchenne et al. 2009]. [Chertok and Keller 2010] treated the tensor as a joint probability of assignments, marginalized the affinity tensor to a matrix, and found optimal soft assignments by eigendecomposition of the matrix. Higher-order assignment problems typically require large amounts of memory and computational resources. By reducing the number of elements needed to represent the affinity measures, the above approaches can match moderate numbers (many hundreds) of features. However, these 2D approaches do not take advantage of supersymmetry of the affinity tensor. SuperMatching does so, leading to an improvement in matching accuracy. 3D problems are even more challenging.

A related idea also using higher order constraints for 3D registration is the 4-points congruent sets method (4PCS) proposed in [Aiger et al. 2008]. It is a fast alignment scheme for 3D point sets that uses widely separated points. However, the need to find coplanar 4-tuples of points and the assumption of rigid transformation limit its applicability. We solve both rigid and isometric shape matching problems with a single approach.

3 Overview

A tensor generalizes vectors and matrices to higher dimensions: a vector is a tensor of order one, and a matrix is a tensor of order two. A higher-order tensor can be expressed as a multi-dimensional array [Kolda and Bader 2009]. More formally, an N^{th} -order tensor is an element of the tensor product of N vector spaces, each with its own coordinate system.

Assume we are given two sets of feature points P_1 and P_2 , with N_1 and N_2 points respectively. $i_n = (f_{i_n}^1, f_{i_n}^2)$ is a pair of points from P_1 and P_2 , respectively. Matching between these two feature sets can be represented by an *assignment variable* x which is a vector $x \in \{0, 1\}^{N_1 N_2}$, with each element representing whether a pair $i_n = (f_{i_n}^1, f_{i_n}^2)$ is selected in the matching (if $x_{i_n} = 1$) or not (if $x_{i_n} = 0$). From the N^{th} -order tensor viewpoint, the matching problem is equivalent to finding the optimal assignment tensor $x^* \in \{0, 1\}^{N_1 N_2}$, satisfying [Kolda and Bader 2009]

$$x^* = \arg \max_x \sum_{i_1, \dots, i_N} \mathcal{T}_N(i_1, \dots, i_N) x_{i_1} \dots x_{i_N}. \quad (1)$$

Here, $i_n \in \{i_1, \dots, i_N\}$ stands for an assignment in the n^{th} dimension of the N vector spaces. Let all feature tuples for P_1 and P_2 be F_1 and F_2 , then $\forall (f_{i_1}^1, \dots, f_{i_N}^1) \in F_1$, there is a matching to corresponding feature tuples in F_2 . For example, given a third-order tensor, $i_n \in \{1, 2, 3\}$, each index could be expressed as $i_1 = (f_{i_1}^1, f_{i_1}^2)$, $i_2 = (f_{i_2}^1, f_{i_2}^2)$, $i_3 = (f_{i_3}^1, f_{i_3}^2)$: pairs of potentially matched points. The product $x_{i_1} \dots x_{i_N}$ will be equal to 1 if the points $(f_{i_1}^1, \dots, f_{i_N}^1)$ are matched to the points $(f_{i_1}^2, \dots, f_{i_N}^2)$, and otherwise 0. $\mathcal{T}_N(i_1, \dots, i_N)$ is the affinity of

the set of assignments $\{i_n\}_{n=1}^N$, which is high if the features in tuple $(f_{i_1}^1, \dots, f_{i_N}^1)$ have similar values to the features in the tuple $(f_{i_1}^2, \dots, f_{i_N}^2)$, and their distance constraints are similar. Note that the size of $\mathcal{T}_N(i_1, \dots, i_N)$ is $(N_1 N_2)^N$. In this paper, the affinity measures expressing similarity of feature tuples are stored using a supersymmetric tensor.

In the rest of the paper, we consider the one-to-many correspondence problem. We assume that each point in P_1 is matched to exactly one point in P_2 , but that the reverse is not necessarily true. If we *do* want to treat both datasets in the same way, we can first match P_1 to P_2 , then match P_2 to P_1 , and then combine the matching results by taking their union or intersection.

From Equ.(1) we can see that there are four issues to be considered when using higher-order matching algorithms. How should we:

- organize and express the affinity measures \mathcal{T}_N in a supersymmetric manner? (see Section 4.1)
- approximately solve the optimal higher-order assignment problem efficiently? (see Section 4.2)
- determine an appropriate sampling strategy to estimate the affinity tensor in a way which will give good matching accuracy (it is too large to compute fully)? (see Section 4.3)
- define a suitable affinity measure between two feature tuples? (see Section 4.4)

4 SuperMatching

We now discuss the first two issues mentioned above, which are independent of application; later we turn to sampling strategy and definition of affinity measure, which is application dependent.

4.1 Supersymmetric Affinity Tensor

The supersymmetric higher-order affinity tensor is invariant under permutation of indices. The main motivation of using supersymmetry is to allow us to avoid redundant storage and computation.

Definition 1 (Supersymmetric Tensor) A tensor is supersymmetric if its entries are invariant under any permutation of its indices [Kofidis and Regalia 2002].

For example, a third-order supersymmetric tensor \mathcal{T}_3 , satisfies the relationships: $\mathcal{T}_3(i_1, i_2, i_3) = \mathcal{T}_3(i_1, i_3, i_2) = \mathcal{T}_3(i_2, i_1, i_3) = \mathcal{T}_3(i_2, i_3, i_1) = \mathcal{T}_3(i_3, i_1, i_2) = \mathcal{T}_3(i_3, i_2, i_1)$.

Definition 2 (Supersymmetric Affinity Tensor) Given two feature sets P_1 and P_2 , with N_1 and N_2 features respectively, the supersymmetric affinity tensor is an N^{th} order I_1, \dots, I_N , non-negative tensor \mathcal{T}_N , for which there exists a set of indices θ_N , and an N^{th} order potential function ϕ_N , such that

$$\mathcal{T}_N(i_1, \dots, i_N) = \begin{cases} \phi_N(\Omega(i_1, \dots, i_N)) & , \forall (i_1, \dots, i_N) \in \theta_N \\ 0 & , \forall (i_1, \dots, i_N) \notin \theta_N \end{cases} \quad (2)$$

where Ω stands for an arbitrary permutation of the vector. θ_N satisfies $i_m \neq i_n \forall (i_1, \dots, i_N) \in \theta_N, \forall i_m \in \{i_1, \dots, i_N\}$ and $\forall i_n \in \{i_1, \dots, i_N\} - \{i_m\}$.

A tensor element with $(i_1, \dots, i_N) \in \theta_N$ is called a *potential element*, while other elements are called *non-potential elements*. A potential element represents one matching result out of all possible matching candidates. Potential elements are further detailed in Section 4.3.

Algorithm 1 Higher-order power iteration solution (with \mathcal{C}_1 norm) for the supersymmetric affinity tensor

Input: N^{th} -order supersymmetric affinity tensor

Output: Unit ℓ^1 -norm vector \mathbf{u}

```

1: Initialize  $\mathbf{v}_0$  to random values in  $[0,1]$ ,  $k = 1$ 
2: repeat
3:   for all  $(i_1, \dots, i_N) \in \theta_N$  do
4:     for all  $m \in \{i_1, \dots, i_N\}$  do
5:        $v_m^{(k)} = (N-1)! \phi_N(i_1, \dots, i_N) 2v_m^{(k-1)} v_{i_1}^{2(k-1)} \dots$ 
          $v_{m-1}^{2(k-1)} v_{m+1}^{2(k-1)} \dots v_{i_N}^{2(k-1)}$ 
6:     end
7:   for  $i = 1 : N_1$  do
8:      $v^{(k)}(((i-1) \cdot N_2 + 1) : i \cdot N_2) =$ 
        $\hat{v}^{(k)}(((i-1) \cdot N_2 + 1) : i \cdot N_2) / \|\hat{v}^{(k)}(((i-1) \cdot N_2 + 1) :$ 
        $i \cdot N_2)\|_1$ 
9:   end
10:  end
11:   $k = k + 1;$ 
12: until convergence;
13:  $\mathbf{u}^{(k)} = \mathbf{v}^{2(k)}$ 
Note:  $\mathbf{u}^{(k)} = \mathbf{v}^{2(k)}$ , and  $v^{(k)}(((i-1) \cdot N_2 + 1) : i \cdot N_2)$  denotes the slice of  $v^{(k)}$  with indices from  $(i-1) \cdot N_2 + 1$  to  $i \cdot N_2$ .
```

Using Definition 2, we can reduce the amount of storage needed, byrepresenting every potential element $\mathcal{T}_N(i_1, \dots, i_N)$ by its canonical entry $\mathcal{T}_N(\text{sort}(i_1, \dots, i_N))$, $\forall (i_1, \dots, i_N) \in \theta_N$. Each stored value thus provides the value for $N!$ entries. Furthermore, as non-potential elements all have value zero, there is no need to store them. This greatly reduces both storage, and the amount of feature tuple sampling needed when estimating the affinity tensor, as discussed in Section 4.3. At the same time, it can be used to make the power iteration process more efficient: see Section 4.2.

4.2 Supersymmetric Higher-order Power Iteration

The higher-order tensor problem in Eq. (1) may be solved by tensor decomposition [Kolda and Bader 2009]; tensor decomposition originated in [Hitchcock 1927]. We utilize the rank-one higher-order power method [Lathauwer et al. 1995] to approximately solve Eq. (1); as noted, an exact computation is infeasible. Eq. (1) can be expressed as:

$$\begin{aligned} \mathbf{x}^* &= \arg \max_{\mathbf{x}} \sum_{i_1, i_2, \dots, i_N} \mathcal{T}_N(i_1, \dots, i_N) x_{i_1} \dots x_{i_N} \\ &= \max \langle \mathcal{T}_N, \mathbf{x}^{\star N} \rangle \end{aligned} \quad (3)$$

where \star is called the Tucker product [Kofidis and Regalia 2002], and $\mathbf{x} \in \{0,1\}^N$. To get an approximate solution, we relax the constraints: the binary assignment vector $\mathbf{x} \in \{0,1\}^N$ is replaced by an assignment vector \mathbf{u} with elements taking real values in $[0,1]$. This changes the optimization problem to one of computing the rank-one approximation of the affinity tensor \mathcal{T}_N [Kofidis and Regalia 2002], i.e. finding a scalar λ and a unit norm vector $\mathbf{u} \in \mathbb{R}^N$, such that the tensor $\hat{\mathcal{T}}_N = \lambda \mathbf{u} \star \dots \star \mathbf{u} = \mathbf{u}^{\star N}$ minimizes the Frobenius norm squared function $f(\hat{\mathcal{T}}_N) = \|\mathcal{T}_N - \hat{\mathcal{T}}_N\|_F^2$. The final matching result is found by replacing each element of \mathbf{u} by 0 or 1 according to whichever it is closer to.

The higher-order power method is commonly used for finding rank-one tensor approximations; a version for supersymmetric tensors (S-HOPM) is given in [Kofidis and Regalia 2002]. The S-HOPM algorithm converges under the assumption of convexity (or concavity) for the functional induced by the tensor [Kofidis and Regalia 2002], which is sufficiently robust for practical applications. S-HOPM is performed in two iterative steps: higher-order power iteration of \mathbf{u} , followed by normalization of \mathbf{u} under the Frobenius

norm. A recent effective improvement [Duchenne et al. 2009] uses the ℓ^1 norm to replace the traditional ℓ^2 norm.

We both use the ℓ^1 norm, and further revise S-HOPM as follows. To perform higher-order power iteration of \mathbf{u} , we must compute

$\hat{\mathbf{u}}^{(k)} = \mathcal{I} \star^{\mathcal{T}_N} (\mathbf{u}^{(k-1)})^{\star^{\mathcal{T}_N} (N-1)}$, where $\star^{\mathcal{T}_N}$ is a so-called \mathcal{T}_N -product, and \mathcal{I} is the unit tensor [Kofidis and Regalia 2002]. For $\hat{\mathbf{u}}^{(k)}$ belonging to an N th-order supersymmetric affinity tensor, this can be formulated as follows:

$$\hat{\mathbf{u}}^{(k)} = \mathcal{I} \star^{\mathcal{T}_N} (\mathbf{u}^{(k-1)})^{\star^{\mathcal{T}_N} (N-1)} \text{ implies that } \forall m \in (i_1, \dots, i_N),$$

$$v_m^{(k)} = \sum_{i_1, \dots, i_N} \mathcal{T}_N(i_1, \dots, i_N) 2v_m^{(k-1)} v_{i_1}^{2(k-1)} \dots v_{i_{m-1}}^{2(k-1)} v_{m+1}^{2(k-1)} \dots v_{i_N}^{2(k-1)} =$$

$$(N-1)! \phi_N(i_1, \dots, i_N) 2v_m^{(k-1)} v_{i_1}^{2(k-1)} \dots v_{i_{m-1}}^{2(k-1)} v_{m+1}^{2(k-1)} \dots v_{i_N}^{2(k-1)} \quad (4)$$

where $\mathbf{u}^{(k)} = \mathbf{v}^{2(k)}$, and ϕ_N is the potential function explained in Section 4.4. Eq. (4) is more compact than earlier expressions in the literature, as it handles all symmetrically related potential elements as a single item using multiplication by $(N-1)!$.

Many initialization schemes have been proposed for the S-HOPM method [Kofidis and Regalia 2002]. We simply use positive random values between 0 and 1 to initialize \mathbf{u}_0 , which ensures convergence; proofs are detailed in [Regalia and Kofidis 2000; Kofidis and Regalia 2002].

Our supersymmetric higher-order power iteration solution of Eq. (1) is performed by the SuperMatching algorithm—see Algorithm 1. Its efficiency relies on two principles. First, we take advantage of the supersymmetry to deduce \mathbf{u} as in Eq. (4), using just a single canonical element for computation (see Step 5). Secondly, power iteration just considers the non-zero potential elements, and excludes each non-potential element from the iteration process. The complexity of the whole iteration process depends only on the number $|\theta_N|$ of non-zero affinities. Consequently, this method reduces also memory costs while keeping accuracy.

Note that, although [Duchenne et al. 2009] claimed to use a supersymmetric affinity tensor, his approach does not make full use of supersymmetry when creating the supersymmetric affinity tensor, nor does it take advantage of supersymmetry to accelerate the power iteration process. By doing so, we overcome limitations due to unbalanced and redundant tensor elements in [Duchenne et al. 2009], as our experiments show later.

4.3 Sampling Strategy

Algorithm 1 depends on the potential elements. We next discuss the issue of how to sample the feature tuples to build potential items, which determines the size $|\theta_N|$ and influences matching accuracy (and speed).

Given the two feature sets P_1 and P_2 , a potential element may be obtained by using a feature tuple sampled from each feature set separately. For N th-order matching, a naive way to construct the potential elements is as follows: first find all feature tuples for P_1 and P_2 , as F_1 and F_2 ; then $\forall (f_{i_1}^1, \dots, f_{i_N}^1) \in F_1$, calculate the potentials for $(f_{i_1}^1, \dots, f_{i_N}^1)$ with all feature tuples in F_2 . This is far too time-consuming, so sampling is used instead. We suggest random sampling for general feature matching problems, but this does not preclude more directed sampling if prior knowledge of the matching problems gives guidance.

Our sampling approach is to repeatedly randomly sample t_1 feature tuples for each feature point from P_1 , and fully sample P_2 . For P_1 , we take each feature in turn as a required element, and then randomly choose t_1 feature tuples containing this required element. Thus, the number of feature tuples in F_1 is $N_1 t_1$, and N_2^N in F_2 . Then, for each feature tuple in F_1 , we find the k most similar features in F_2 to build k potential elements as ϕ_i^k . Combining all the potential elements obtained, we form the desired potential element set $\theta_N = \{\phi_i^k\}_{i=1}^{N_1 t_1 k}$, of size $|\theta_N| = N_1 t_1 k$. For P_1 , the sampling cost is $O(N_1 t_1 k \log N_2)$, where $\log N_2$ is coming from the KD-tree cost for the searching k most similar features in F_2 . The parameters t_1 and k must be chosen according to the size of the feature sets. In practice, for two feature sets each with hundreds of points, we may take $t_1 \approx 100$ and $k \approx 300$ for third-order matching. Our experiments demonstrate that this sampling approach works well.

An important aspect of our sampling approach is to use the supersymmetry of the affinity tensor. Potential elements whose indices are permutations of each other have the same value, so should not be repeatedly sampled. Thus, we use a sampling constraint that the sets of feature tuples F_1 obtained from the sampling process should have no repetition, in the sense that

$$\forall (f_{i_1}^1, f_{i_2}^1, \dots, f_{i_N}^1), (f_{j_1}^1, f_{j_2}^1, \dots, f_{j_N}^1) \in F_1,$$

$$(f_{i_1}^1, f_{i_2}^1, \dots, f_{i_N}^1) \neq \Omega(f_{j_1}^1, f_{j_2}^1, \dots, f_{j_N}^1) \quad (5)$$

where Ω is an arbitrary permutation.

Earlier work [Zass and Shashua 2008; Duchenne et al. 2009; Wang et al. 2010] adopted random sampling, but failed to impose any constraint on the sampling process to take into account supersymmetry, leading to the possibility that feature tuples may be sampled multiple times. For example, for third-order matching, it is possible that a feature tuple $(f_{i_1}^1, f_{i_2}^1, f_{i_3}^1)$ may be sampled from P_1 and $(f_{i_1}^2, f_{i_2}^2, f_{i_3}^2)$ from P_2 , and also a feature tuple $(f_{i_1}^1, f_{i_3}^1, f_{i_2}^1)$ from P_1 and $(f_{i_1}^2, f_{i_3}^2, f_{i_2}^2)$ from P_2 . That would create two tensor elements $\phi_3(i_1, i_2, i_3)$ with index (i_1, i_2, i_3) and $\phi_3(i_1, i_3, i_2)$ with index (i_1, i_3, i_2) , which are the same. However, we just need one tensor element to express the affinity on the assignment group (i_1, i_2, i_3) for any permutation of indices. This extra sampling is not only inefficient, but may also reduce the accuracy of the power iteration: one set of symmetrically related elements may be represented by a different number of samples than another set of symmetrically related elements, which unbalances the power iteration process, and can lead to inaccurate results. Our sampling method reduces the sampling cost, while also improving the accuracy of the power iteration.

4.4 Higher-order Potentials

Different higher-order potentials are appropriate for different applications. Here we briefly give two simple examples of general higher-order potentials for 2D and 3D matching respectively; we use them later to evaluate our algorithm. The potentials are based on a Gaussian function which guarantees the tensor elements are non-negative and invariant under any permutation of the input assignments.

In 2D, we use a well-known third-order geometric-similarity invariant potential ϕ_3 [Duchenne et al. 2009; Chertok and Keller 2010] for linking point feature triples. Triangles formed by three points are *similar* under scaling, rotation and translation—interior angles are invariant. Thus ϕ_3 can be defined in terms of differences of corresponding interior angles:

$$\phi_3(i_1, i_2, i_3) = \phi_3(\{p_1, q_1\}, \{p_2, q_2\}, \{p_3, q_3\})$$

$$= \exp(-1/\varepsilon^2 \sum_{(l,l')} \|\alpha_l - \alpha_{l'}\|^2) \quad (6)$$

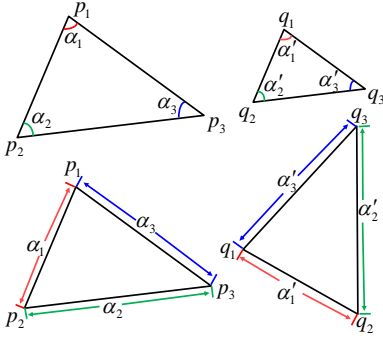


Figure 2: Third-order potential. The geometric constraints are: internal angle invariance in 2D (above), and edge length invariance in 3D (below).

where $\varepsilon > 0$ is the kernel bandwidth, which is automatically computed as the average the ℓ^1 norm of all differences, and $\{\alpha_l\}_{l=1}^3$ and $\{\alpha'_l\}_{l=1}^3$ are the angles formed by feature triples (p_1, p_2, p_3) and (q_1, q_2, q_3) : see Figure 2. Each point corresponds to one interior angle. We may extend it to higher order by using the internal angles formed by polygons with more than 3 sides.

For 3D matching problems, we may replace the internal angles by edge lengths, which for meshes are based on geodesic distance across the mesh in which the points are embedded. This corresponds to assuming an isometry transform relating the meshes. Geodesic distance may be computed by Dijkstra’s algorithm [Peyré et al. 2010]. See Figure 2.

5 Experiments

We have used synthetic data and real captured data to evaluate the SuperMatching algorithm. To demonstrate the SuperMatching algorithm’s independence of feature descriptors, several descriptors were used. In some cases, we simply uniformly sampled feature points on the objects, and used a trivial feature descriptor of 1 for all points, meaning affinities are based simply on distances between feature points—this allows us to show our method is robust in the presence of ambiguous feature descriptors. In other cases, we still used uniformly distributed feature points, together with SIFT descriptors, which shows that feature points do not have to be carefully chosen. We used third-order matching in our experiments, but it would be simple (but more costly) to use higher order.

5.1 3D Rigid Shapes Scans

Firstly, we used SuperMatching to build pairwise matchings between 3D rigid shape scans based on uniformly sampled feature points. Rigid transforms can be computed from each triple of compatible matching points. The transform which brings the most data points within a threshold distance of a point in the model is chosen as the optimal alignment transform [Huttenlocher and Ullman 1990]. As discussed in [Gelfand et al. 2005], such a voting scheme is guaranteed to find the optimal alignment between pairwise scans and is robust to the initial pose of the input scans. Figure 3 shows some registration results for the Rooster model from [Chuang et al. 2009]. The left column shows the original state, the two middle columns are our matching and alignment results, and the right column shows the corresponding result produced by [Aiger et al. 2008], which has clearly failed, presumably as only 4 points were used to deduce the alignment. We compared the transformation matrix computed by the SuperMatching with the ground truth provided

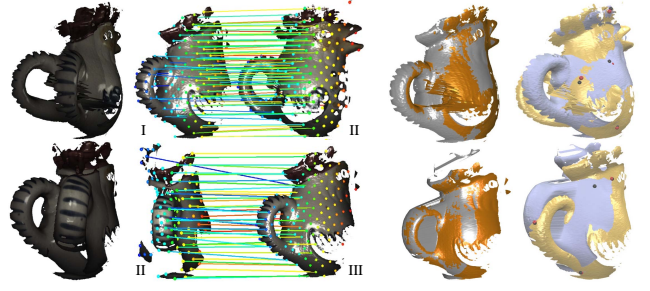


Figure 3: Pairwise alignment of Rooster I – II and II – III scans. From left to right: before alignment, our matching result, our alignment result, alignment result from [Aiger et al. 2008].

Table 1: Transformation matrix comparison

	computed matrix				ground truth			
I	0.706748	-0.004298	-0.705324	-131.983	0.707322	-0.004322	-0.706878	-132.334
—	-0.012433	1.000000	-0.01300	-3.40032	-0.0115584	0.999777	-0.0176787	-3.31322
II	0.711232	0.019837	0.700231	-55.0001	0.706797	0.0206749	0.707114	-54.1285
—	0	0	0	1	0	0	0	1
I	0.000743	-0.022132	-1.000000	-188.032	0.000735502	-0.021993	-0.999758	-187.661
—	-0.031999	1.000000	-0.022000	-4.12834	-0.0322266	0.999238	-0.0220053	-4.1392
III	1.000000	0.031897	0.0000026	-185.893	0.99948	0.032235	2.61817e-05	-186.005
—	0	0	0	1	0	0	0	1

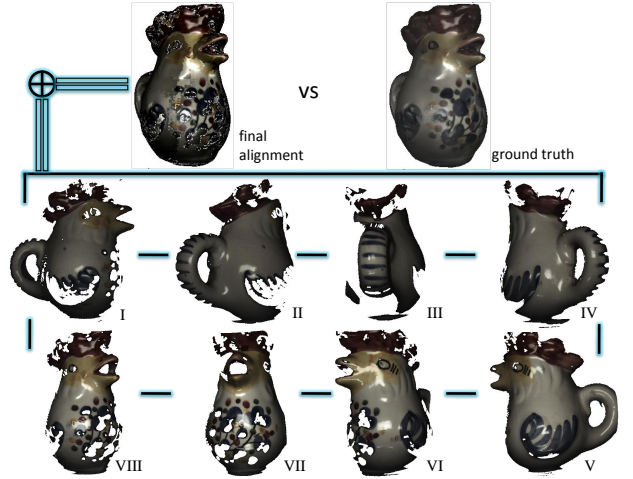


Figure 4: Alignment of several Rooster scans from different viewpoints. Above: our final registered Rooster and the ground truth [Chuang et al. 2009]. Below: 8 partial scans, the dark lines indicating the pairwise matches.

by [Chuang et al. 2009]. Table 1 demonstrates that our computed matrices for I-II and I-III are so similar with the ground truth.

Next, we used SuperMatching to build a complete model from a set of scans from different viewpoints. For these multiple scans, third-order matching was first performed between each pair of consecutive scans. After doing so, the alignment was refined using the iterative closest point (ICP) algorithm [Besl and McKay 1992]. Figure 4 illustrates the approach and shows the result.

5.2 3D Depth Scans with Color Information

We next provide a further real-world, noisy, example of the use of SuperMatching. In this case, data with surface color information

was captured using a Kinect camera. [Kinect 2012], Uniform samples and SIFT feature vectors were used as a basis for SuperMatching. This resulted in robust matches without significant outliers, as illustrated in Figure 5.

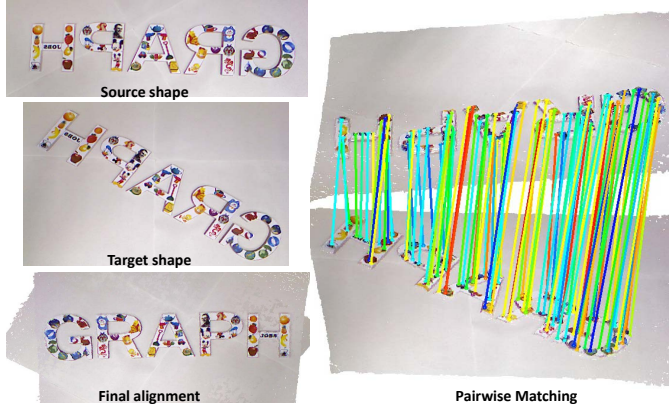


Figure 5: 3D real depth scans with color information, captured using Kinect. Matching points are connected by colored lines.

5.3 3D Articulated Shape Synthetic Data

A further application is registration of (approximately) articulated shapes. Such problems are common in dynamic range scanning such as human motion capture. Given a sequence of range scans of a moving articulated subject, our method automatically registers all data to produce a complete 3D shape. Unlike many other methods, we do not need manual segmentation, markers, or a prior template. While the problem of non-rigid registration of deformable shapes is ill-posed and no algorithm is applicable to all scenarios, we believe that our approach pushes the limits of what can be achieved with minimal prior information. SuperMatching provides robust, accurate matching, even although the partial scans have holes and different poses.

Again uniformly sampled points were used. Registration of scans was performed by computing piecewise rigid transformations between matches. These transformations may be propagated from feature points to the entire set of points in each scan using nearest neighbor interpolation. Figure 6 shows a registration example for an articulated model. On the left is our result, on the right is the result produced by the method [Chang and Zwicker 2009].

For a sequence of partial articulated data, registration is performed in two main steps. We first precompute an initial pairwise registration for each pair of consecutive frames, then perform articulated shape reconstruction as in [Pekelnny and Gotsman 2008]. Segmentation of the scans into rigid parts can readily be done by clustering the transformations obtained from uniformly feature points, using the mean shift algorithm [Comaniciu and Meer 2002]. This information is used as input to the second step of articulated shape reconstruction following [Pekelnny and Gotsman 2008]; this algorithm identifies and tracks the rigid parts in each frame, while accumulating geometric information over time. However, [Pekelnny and Gotsman 2008] requires the user to manually segment each range scan in advance, whereas we automatically determine the segmentation. Figure 7 shows an articulated hand example. This synthetic data is generated from a deformation sequence, and the final registered shape is produced from these partial data. By using synthetic data, we are able to evaluate the robustness of our reconstruction method using the ground truth, as shown in Figure 7. Quantitatively, we measured the maximum of the average distance of the reconstruc-

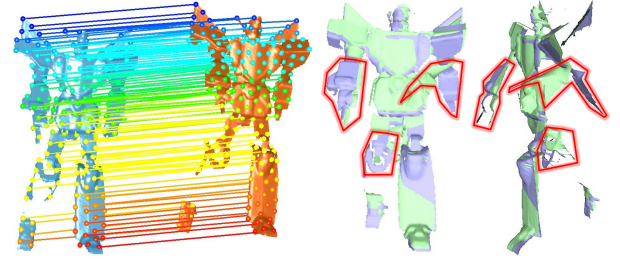


Figure 6: Pairwise matching of an articulated Robot between two frames. Left: our result. Right: result produced by [Chang and Zwicker 2009], from front and side views; red polygons indicate regions of large distortion.

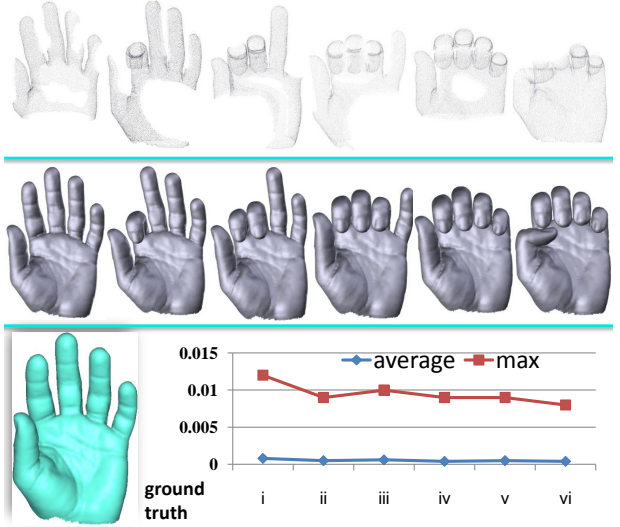


Figure 7: Registration of an articulated hand. Above: partial synthetic data with holes generated from a deformation sequence. Middle: reconstructed meshes are deduced from the registration process. Below: first frame ground truth shape, and average and maximum distance from the ground truth per frame.

tion over all frames as $0.001D$ where D is the bounding box diagonal length, and the greatest distance error in any one frame was $0.012D$.

5.4 Deformable Surfaces

Finally, we matched SIFT points on images of deforming surfaces¹ showing a cloth and a cushion. The surface of the cloth underwent relatively smooth deformation, while the surface of the cushion included sharp folds. This data comes with ground truth, which allows quantitative verification of the accuracy of the matches found. From each surface set we randomly chose two frames before and after a large deformation. We randomly chose 100 corresponding points on each surface, using the provided ground truth.

We used the above input data as a basis for comparison with the spectral algorithm [Cour et al. 2006] (a quadratic assignment algorithm), a third-order tensor algorithm [Duchenne et al. 2009], and the hypergraph matching algorithm [Zass and Shashua 2008], using the authors' code in each case. All methods were executed in Matlab on a 2.3GHz Core2Duo with 2GB memory. To enable direct

¹From <http://cvlab.epfl.ch/data/dsr/>

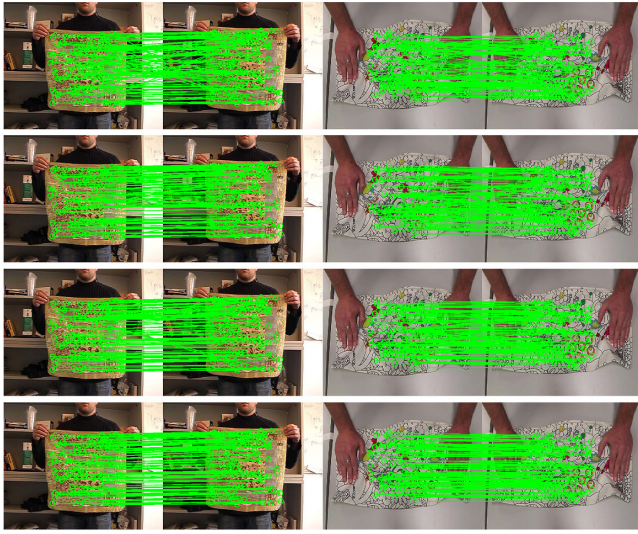


Figure 8: Matching results. Left: cloth set, matching between frame 80 and 90, right: cushion set, matching between 144 and 156. Top to bottom, spectral method [Cour et al. 2006], hypergraph matching method [Zass and Shashua 2008], a third-order tensor method [Duchenne et al. 2009], and SuperMatching.

and fair comparison, [Duchenne et al. 2009], [Zass and Shashua 2008] and SuperMatching used the same potential and the same tensor size.

In these tests, SuperMatching considered 3×10^6 feature tuples, while the method of [Duchenne et al. 2009] considered 10×10^6 tuples and the method of [Zass and Shashua 2008] used 4×10^6 . The difference mainly results from differences in sampling strategy; note that we have the lowest sampling cost. The average running time to match two feature sets each with 100 features was around 8s for SuperMatching, 13s for [Duchenne et al. 2009], 6.5s for [Zass and Shashua 2008], and 5s for [Cour et al. 2006]. SuperMatching takes less time than the third-order tensor algorithm in [Duchenne et al. 2009] both because it uses fewer feature tuples and because of the more efficient supersymmetric higher-order power iteration solution.

Matching accuracy was assessed by the number of correctly matched points (known from the ground truth) divided by the total number of points that could be matched. The results are summarised in Table 2 and illustrated in Figure 8. Table 2 demonstrates that SuperMatching achieves a higher matching accuracy than previous algorithms. The worst matching result is produced by the spectral quadratic assignment algorithm [Cour et al. 2006], due to the lower discriminatory power of pairwise geometric constraints. Higher-order algorithms perform better due to the more complex geometric constraints. Nevertheless, SuperMatching also significantly outperforms the third-order algorithm [Duchenne et al. 2009] and the hypergraph matching algorithm [Zass and Shashua 2008], as these do not take proper advantage of supersymmetry.

6 Conclusions

This paper has presented the SuperMatching algorithm, which tackles the classic computer graphics and computer vision problem of feature matching, independently of feature description. It is an efficient higher-order matching algorithm which uses a compact form of the higher-order supersymmetric affinity tensor to express relatedness of features. Matching is performed using an efficient

Table 2: Accuracy of deformable surface matching.

Dataset	cloth					cushion				
Matching frames	F80- F90- F95- F100- F90 F95 F100 F105	F144- F156- F165- F172- F156 F165 F172 F188								Time (s)
SuperMatching	83% 85% 84% 81%	66% 60% 69% 56%								8
[Zass and Shashua 2008]	73% 79% 70% 72%	44% 39% 54% 43%								6.5
[Duchenne et al. 2009]	67% 77% 73% 65%	39% 31% 47% 42%								13
[Cour et al. 2006]	27% 29% 22% 27%	14% 5% 28% 7%								5

power iteration method, which takes advantage of supersymmetry and avoids computing with zero elements. We also give an efficient sampling strategy for choosing feature tuples to create the affinity tensor. Experiments on both synthetic and real 2D and 3D data sets show that SuperMatching has greater accuracy than competing methods, whilst having competitive performance.

In future, we wish to further improve the performance of the SuperMatching algorithm. Random sampling could be executed in parallel, for example. We also intend to apply it to more challenging deformable imperfect 3D data matching with real captured data. SuperMatching has applicability to many fields, as matching is a foundation for many computer graphics and computer vision applications.

Acknowledgements. We are grateful to [omitted for review] for sharing source code, executable programs, and test data. SuperMatching source code [will be] publicly available under the GNU Lesser General Public License from [omitted for review].

References

- AIGER, D., MITRA, N. J., AND COHEN-OR, D. 2008. 4-points congruent sets for robust pairwise surface registration. *ACM Transactions on Graphics* 27, 3.
- BERG, A. C., BERG, T. L., AND MALIK, J. 2005. Shape matching and object recognition using low distortion correspondence. In *IEEE CVPR*, 26–33.
- BESL, P. J., AND MCKAY, N. D. 1992. A method for registration of 3-d shapes. *IEEE Transactions on Pattern Analysis and Machine Intelligence* 14, 239–256.
- BRONSTEIN, A. M., BRONSTEIN, M. M., GUIBAS, L. J., AND OVSJANIKOV, M. 2011. Shape google: Geometric words and expressions for invariant shape retrieval. *ACM Transactions on Graphics* 30, 1:1–1:20.
- BROWN, B. J., AND RUSINKIEWICZ, S. 2007. Global non-rigid alignment of 3-d scans. *ACM Transactions on Graphics* 26.
- CHANG, W., AND ZWICKER, M. 2009. Range scan registration using reduced deformable models. *Computer Graphics Forum (Proc. Eurographics)* 28, 2, 447–456.
- CHANG, W., AND ZWICKER, M. 2011. Global registration of dynamic range scans for articulated model reconstruction. *ACM Transactions on Graphics* 30, 26:1–26:15.
- CHERTOK, M., AND KELLER, Y. 2010. Efficient high order matching. *IEEE Transactions on Pattern Analysis and Machine Intelligence* 32, 2205–2215.
- CHUANG, M., LUO, L., BROWN, B. J., RUSINKIEWICZ, S., AND KAZHDAN, M. M. 2009. Estimating the laplace-beltrami operator by restricting 3d functions. *Computer Graphics Forum (Proc. SGP)* 28, 5, 1475–1484.

- COMANICIU, D., AND MEER, P. 2002. Mean shift: A robust approach toward feature space analysis. *IEEE Transactions on Pattern Analysis and Machine Intelligence* 24, 603–619.
- CONTE, D., FOGGIA, P., SANSONE, C., AND VENTO, M. 2004. Thirty years of graph matching in pattern recognition. *International Journal of Pattern Recognition and Artificial Intelligence* 18, 3, 265–298.
- COUR, T., SRINIVASAN, P., AND SHI, J. 2006. Balanced graph matching. In *NIPS*, 313–320.
- DUCHENNE, O., BACH, F., KWEON, I., AND PONCE, J. 2009. A tensor-based algorithm for high-order graph matching. In *IEEE CVPR*, 1980–1987.
- GELFAND, N., MITRA, N. J., GUIBAS, L. J., AND POTTSMANN, H. 2005. Robust global registration. In *Symposium on Geometry processing*.
- HITCHCOCK, F. L. 1927. The expression of a tensor or a polyadic as a sum of products. *Journal of Mathematics and Physics* 6, 064–089.
- HUTTENLOCHER, D. P., AND ULLMAN, S. 1990. Recognizing solid objects by alignment with an image. *International Journal of Computer Vision* 5 (November), 195–212.
- JOHNSON, A. E., AND HEBERT, M. 1999. Using spin images for efficient object recognition in cluttered 3d scenes. *IEEE Transactions on Pattern Analysis and Machine Intelligence* 21, 5, 433–449.
- KIM, V. G., LIPMAN, Y., AND FUNKHOUSER, T. 2011. Blended intrinsic maps. In *SIGGRAPH*, 79:1–79:12.
- KINECT, 2012. Kinect homepage. <http://www.xbox.com/en-US/kinect>.
- KOFIDIS, E., AND REGALIA, P. A. 2002. On the best rank-1 approximation of higher-order supersymmetric tensors. *SIAM Journal on Matrix Analysis and Applications* 23, 3, 863–884.
- KOLDA, T. G., AND BADER, B. W. 2009. Tensor decompositions and applications. *SIAM Review* 51, 3, 455–500.
- LATHAUWER, L. D., COMON, P., MOOR, B. D., AND VANDEWALLE, J. 1995. Higher-order power method. In *Proceedings of NOLTA*, 2709–2712.
- LEORDEANU, M., AND HEBERT, M. 2005. A spectral technique for correspondence problems using pairwise constraints. In *International Conference of Computer Vision*, 1482–1489.
- LEUTENEGGER, S., CHLI, M., AND SIEGWART, R. 2011. Brisk: Binary robust invariant scalable keypoints. In *International Conference of Computer Vision*.
- LI, H., SUMNER, R. W., AND PAULY, M. 2008. Global correspondence optimization for non-rigid registration of depth scans. *Computer Graphics Forum (Proc. SGP)* 27, 5, 1421–1430.
- LIPMAN, Y., AND FUNKHOUSER, T. 2009. Möbius voting for surface correspondence. *ACM Transactions on Graphics (Proc. SIGGRAPH)* 28, 72:1–72:12.
- LOWE, D. G. 2004. Distinctive image features from scale-invariant keypoints. *International Journal of Computer Vision* 60, 91–110.
- OVSIJANIKOV, M., MRIGOT, Q., MMOLI, F., AND GUIBAS, L. 2010. One point isometric matching with the heat kernel. *Computer Graphics Forum (Proc. SGP)* 29, 5, 1555–1564.
- PEKELNY, Y., AND GOTSMAN, C. 2008. Articulated object reconstruction and markerless motion capture from depth video. *Computer Graphics Forum (Proc. EuroGraphics)* 27, 2, 399–408.
- PEYRÉ, G., PÉCHAUD, M., KERIVEN, R., AND COHEN, L. D. 2010. Geodesic methods in computer vision and graphics. *Foundations and Trends in Computer Graphics and Vision* 5, 197–397.
- REGALIA, P. A., AND KOFIDIS, E. 2000. The higher-order power method revisited: convergence proofs and effective initialization. In *Proceedings of the Acoustics Speech and Signal Processing*, IEEE Computer Society, 2709–2712.
- SAHILLIOGLU, Y., AND YEMEZ, Y. 2011. Coarse-to-fine combinatorial matching for dense isometric shape correspondence. *Computer Graphics Forum (Proc. SGP)* 30, 5, 1461–1470.
- SUN, J., OVSIJANIKOV, M., AND GUIBAS, L. 2009. A concise and provably informative multi-scale signature based on heat diffusion. In *Symposium on Geometry Processing*, 1383–1392.
- SUN, J., CHEN, X., AND FUNKHOUSER, T. A. 2010. Fuzzy geodesics and consistent sparse correspondences for deformable shapes. *Computer Graphics Forum* 29, 5, 1535–1544.
- TEVS, A., BOKELOH, M., WAND, M., SCHILLING, A., AND SEIDEL, H.-P. 2009. Isometric registration of ambiguous and partial data. In *IEEE CVPR*, 1185–1192.
- TEVS, A., BERNER, A., WAND, M., IHRKE, I., AND SEIDEL, H.-P. 2011. Intrinsic shape matching by planned landmark sampling. *Computer Graphics Forum* 30, 2, 543–552.
- TOLER-FRANKLIN, C., BROWN, B., WEYRICH, T., FUNKHOUSER, T., AND RUSINKIEWICZ, S. 2010. Multi-feature matching of fresco fragments. *ACM Transactions on Graphics (Proc. SIGGRAPH ASIA)* 29, 185:1–185:12.
- TORRESANI, L., KOLMOGOROV, V., AND ROTHER, C. 2008. Feature Correspondence Via Graph Matching: Models and Global Optimization. In *the 10th European Conference on Computer Vision*, Springer-Verlag, 596–609.
- VAN KAICK, O., ZHANG, H., HAMARNEH, G., AND COHEN-OR, D. 2011. A survey on shape correspondence. *Computer Graphics Forum* 30, 6, 1681–1707.
- WAND, M., ADAMS, B., OVSIJANIKOV, M., BERNER, A., BOKELOH, M., JENKE, P., GUIBAS, L., SEIDEL, H.-P., AND SCHILLING, A. 2009. Efficient reconstruction of nonrigid shape and motion from real-time 3d scanner data. *ACM Transactions on Graphics* 28, 15:1–15:15.
- WANG, A., LI, S., AND ZENG, L. 2010. Multiple order graph matching. In *Asian Conference on Computer Vision*, 471–482.
- WINDHEUSER, T., SCHLICKWEI, U., SCHIMDT, F. R., AND CREMERS, D. 2011. Large-scale integer linear programming for orientation preserving 3d shape matching. *Computer Graphics Forum (Proc. SGP)* 30, 5, 1471–1480.
- ZASS, R., AND SHASHUA, A. 2008. Probabilistic graph and hypergraph matching. In *IEEE CVPR*, 1–8.
- ZENG, Y., WANG, C., WANG, Y., GU, X., SAMARAS, D., AND PARAGIOS, N. 2010. Dense non-rigid surface registration using high-order graph matching. In *IEEE CVPR*, 382–389.